

1 Title: SARS-CoV-2 infection severity is linked to superior humoral immunity against the spike

2

3 Jenna J. Guthmiller^{1,12*}, Olivia Stovicek^{1,12}, Jiaolong Wang^{1,12}, Siriruk Changrob¹, Lei Li¹, Peter
4 Halfmann², Nai-Ying Zheng¹, Henry Utset¹, Christopher T. Stamper³, Haley L. Dugan³, William D.
5 Miller⁴, Min Huang¹, Ya-Nan Dai⁵, Christopher A. Nelson⁵, Paige D. Hall⁵, Maud Jansen⁶, Kumaran
6 Shanmugarajah⁷, Jessica S. Donington⁷, Florian Krammer⁸, Daved H. Fremont⁵, Andrzej
7 Joachimiak^{9,10}, Yoshihiro Kawaoka², Vera Tesic¹¹, Maria Lucia Madariaga⁷, Patrick C. Wilson^{1,3*}

8

9 ¹Department of Medicine, Section of Rheumatology, University of Chicago, Chicago, IL 60637, USA

10 ²Influenza Research Institute, Department of Pathobiological Sciences, School of Veterinary Medicine,
11 University of Wisconsin-Madison, Madison, WI, 53711

12 ³Committee on Immunology, University of Chicago, Chicago, IL 60637, USA

13 ⁴Department of Medicine, Section of Pulmonary and Critical Care Medicine, University of Chicago,
14 Chicago, IL 60637, USA

15 ⁵Department of Pathology and Immunology and Center for Structural Genomics of Infectious
16 Diseases, Consortium for Advanced Science and Engineering, Washington University School of
17 Medicine, St. Louis, MO 63110, USA

18 ⁶Department of Medicine, University of Chicago, Chicago, IL 60637, USA

19 ⁷Department of Surgery, University of Chicago, Chicago, IL 60637, USA

20 ⁸Department of Microbiology, Icahn School of Medicine at Mount Sinai, New York, NY 10029, USA

21 ⁹Center for Structural Genomics of Infectious Diseases, Consortium for Advanced Science and
22 Engineering, University of Chicago, Chicago, IL 60667

23 ¹⁰Structural Biology Center, X-ray Science Division, Argonne National Laboratory, Argonne, IL 60439,
24 USA

25 ¹¹Department of Pathology, University of Chicago, Chicago, IL 60637, USA

26 ¹²These authors contributed equally

27 *Correspondence: jguthmiller@uchicago.edu; wilsonp@uchicago.edu

28 ABSTRACT: Severe acute respiratory syndrome coronavirus 2 (SARS-CoV-2) is currently causing a
29 global pandemic. The antigen specificity and kinetics of the antibody response mounted against this
30 novel virus are not understood in detail. Here, we report that subjects with a more severe SARS-CoV-
31 2 infection exhibit a larger antibody response against the spike and nucleocapsid protein and epitope
32 spreading to subdominant viral antigens, such as open reading frame 8 and non-structural proteins.
33 Subjects with a greater antibody response mounted a larger memory B cell response against the
34 spike, but not the nucleocapsid protein. Additionally, we revealed that antibodies against the spike are
35 still capable of binding the D614G spike mutant and cross-react with the SARS-CoV-1 receptor
36 binding domain. Together, this study reveals that subjects with a more severe SARS-CoV-2 infection
37 exhibit a greater overall antibody response to the spike and nucleocapsid protein and a larger memory
38 B cell response against the spike.

39

40

41 Entry of SARS-CoV-2 into host cells is mediated by surface trimeric spike protein via interaction
42 between the spike receptor-binding domain (RBD) and angiotensin-converting enzyme 2^{1,2}. SARS-
43 CoV-2 expresses numerous potential antigens, including four structural proteins (spike, nucleocapsid
44 (N) protein, matrix and envelope protein), 16 nonstructural proteins/antigens (NSP1–NSP16), and
45 several accessory open reading frame (ORF) proteins, including ORF7 and ORF8^{3,4}. To date, little is
46 known about the specificities and kinetics of antibodies elicited in response to this infection and how
47 coronavirus disease 2019 (COVID-19) severity relates to magnitude of the humoral immune
48 response.

49 To address this critically important knowledge gap, we collected plasma samples from 35
50 hospitalized acutely SARS-CoV-2 infected subjects and 105 convalescent subjects⁵ (Supplemental
51 Tables 1 and 2). Plasma was tested against the spike, N protein, ORF7a, ORF8, and NSP3, NSP9,
52 NSP10, and NSP15 of SARS-CoV-2. Notably, all subjects within the acutely infected cohort were
53 hospitalized, whereas only 9% (8/105) of subjects in the convalescent cohort had been hospitalized
54 (Supplemental Tables 1 and 2). 89% of acutely infected subjects and 98% of convalescent subjects
55 had detectable antibodies against one or more SARS-CoV-2 antigens (Fig. 1a), with nearly all
56 subjects mounting a response against the spike and N protein (Fig. 1b). We further identified that
57 convalescent subjects mounted a predominant response against the RBD of the spike protein and the
58 RNA-binding domain of the N protein (Extended data Fig. 1a and b), suggesting these domains
59 contain the immunodominant epitopes of these antigens. A larger frequency of acutely infected
60 subjects mounted antibodies against ORF7a, ORF8, and NSP antigens (Fig. 1b, Extended data Fig.
61 1c) suggesting antibodies against these antigens are either short-lived or only induced by more
62 severe infection. Moreover, the anti-N protein antibody response preceded the antibody response
63 against the spike protein and was consistently higher across all time points, peaking between the 2nd
64 and 3rd week after the onset of symptoms and retracting between the 3rd and 4th weeks after symptom
65 onset (Fig. 1c and Extended data Fig. 1d). Furthermore, we found a strong positive correlation
66 between the anti-N protein and anti-spike IgG titers in both the acutely infected and convalescent
67 cohorts (Extended data 1e and f), indicating subjects who generally mounted a robust antibody

68 response upon SARS-CoV-2 infection tended to mount a robust response against both antigens.
69 Titors against both the spike and N protein persisted even 2+ months after symptom onset (Fig. 1c),
70 indicating the antibody response against these two antigens is stable amongst subjects with
71 symptomatic infection, a finding consistent with other reports^{6,7}. We did not observe a statistical
72 difference in antibody titers against the spike and N protein by individual subjects in either the acute or
73 convalescent subject cohorts (Fig. 1d and e), likely due to dramatic subject-to-subject variation.
74 However, antibody titers against the spike and N protein were significantly higher than antibody titers
75 against ORF7a and ORF8 (Fig. 1d and e). Together, these data reveal the antibody response against
76 SARS-CoV-2 is largely driven against the spike and N protein and that the anti-N protein antibody
77 response precedes the response against the spike. The differences in the kinetics and magnitude of
78 the N protein response are potentially due to the differences in protein expression, as N protein
79 completely covers the entire viral genome, whereas a single virion only expresses ~26 trimers⁸.

80 To understand the inter-subject variability within our cohorts, we performed hierarchical
81 clustering of subjects based on antibody titers against the spike, full length and RNA-binding domain
82 of N protein, ORF7a, and ORF8 antigens. From the acutely infected cohort, we identified three
83 clusters: high, mid, and low responders (Fig. 2a and Supplemental Table 3). Notably, the high
84 responder cluster subjects were further from the onset of symptoms at the time of sampling and
85 ultimately were hospitalized for a longer duration than those in the mid and low responder groups (Fig.
86 2b and c). We did not observe a statistical difference in age or sex between the three responder
87 groups (Extended data Fig. 2a and b). Over 25% of subjects in the high responder group had a
88 severe/highest CURB-65 score (Extended data Fig. 2c), a measure of pneumonia severity⁹,
89 suggesting subjects in the high responder group had more severe infections. We further examined
90 which features of the humoral immune response were driving subjects to segregate into these three
91 clusters. Subjects within the high and mid responder groups robustly induced antibodies against the
92 spike protein, but the high responder subjects mounted a larger response to N protein relative to the
93 mid responder subjects (Fig. 2d-f). Additionally, subjects within the high and mid responder groups
94 were more likely to mount an antibody response against ORF8 and NSP antigens (Extended data Fig.

95 2d and e). The low responder group largely did not mount an antibody response against any of the
96 antigens tested (Fig. 2d-f and Extended Data Fig. 2d and e), although it is possible that plasma was
97 collected before the subjects mounted a significant antibody response. Our data reveal that acutely
98 infected subjects who were hospitalized for a longer duration mounted a larger antibody response
99 against N protein and were more likely to mount a response against other SARS-CoV-2 antigens.

100 The convalescent cohort also clustered into three distinct clusters based on the magnitude of
101 the antibody response against the spike and N protein (Fig. 3a and Supplemental Table 4), similar to
102 the acutely infected cohort (Fig. 2). To understand the relationship between infection severity and
103 antibody responses within the convalescent cohort, we scored subjects based on the severity and
104 duration of self-reported symptoms and whether subjects were hospitalized (Supplemental Table 5).
105 Notably, over 50% of subjects within the high responder group had a severe infection (Fig. 3b and
106 Extended data Fig. 3a), indicating infection severity is linked to increased antibody titers. Moreover,
107 subjects within the high responder group typically were older and male (Fig. 3c and d). Subjects within
108 each responder group had a similar duration of symptoms (Extended data Fig. 3b), and subjects
109 within all three groups had a similar amount of time to mount a response, as determined by the
110 number of days since symptoms onset at the time of donation (Extended data Fig. 3c). Unlike the
111 acutely infected cohort, subjects within the high responder group had higher titers against not only the
112 N protein, but also the spike and ORF8 antigens relative to subjects within the mid and low responder
113 groups (Fig. 3e and f, Extended data Fig. 3d and e), and were trending to be more likely to
114 seroconvert against at least one of the NSP antigens tested (Extended data Fig. 3f). Consistent with
115 these data, high and mid responder subjects had higher neutralizing titers than subjects in the low
116 responder cohorts (Fig. 3g). In combination with the acutely infected cohort, our data reveal subjects
117 with more severe infection are mounting a larger antibody response at both acute and convalescent
118 time points.

119 We next dissected the specificities of memory B cells (MBCs) induced by SARS-CoV-2
120 infection by performing B cell ELISpots on polyclonally stimulated peripheral blood mononuclear cells
121 (PBMCs) isolated from convalescent subjects. Notably, MBCs largely targeted the spike, whereas

122 very few MBCs targeted N protein or ORF8 (Fig. 4a). Additionally, subjects in the serum high
123 responder group mounted a larger MBC response against the spike than subjects in the mid and low
124 responder cohorts (Fig. 4b), with serum antibody titers against the spike positively correlating with the
125 magnitude of the anti-spike MBC response (Fig. 4c). Despite the observed differences in anti-spike
126 MBC responses between responder groups, we did not observe any differences in the anti-N protein
127 and anti-ORF8 MBC response in the three responder cohorts (Extended data Fig. 4a and b).
128 Together, these data indicate that the MBC response is largely directed against the spike protein, and
129 that the high serum responder group mounted both a larger secreted antibody and MBC response
130 upon SARS-CoV-2 infection.

131 SARS-CoV-2 has acquired a D614G mutation within the spike protein and viruses carrying this
132 mutation have since become the dominant circulating strain globally as of early April¹⁰. This mutation
133 is located on the interface between two subunits of the spike trimer and may impact stability of the
134 trimer¹. As the subjects within our study were initially infected throughout March and into early April
135 (Supplemental Tables 1 and 2), they were likely infected with the D614 variant. We did not observe a
136 difference in antibody titers against the WT and D614G spike antigens within our acute cohort (Fig.
137 5a), suggesting the D614G epitope was not a major antigenic site. Strikingly, we identified that the
138 convalescent cohort mounted a larger response against the G614 variant than the WT D614 that they
139 were likely infected with (Fig. 5b), potentially due to the increased stability of the G614 variant¹¹.
140 Furthermore, we observed a strong positive correlation between D614 (WT) spike titers and G614
141 titers, indicating antibodies against the WT strain likely protect against the new G614 variant (Fig. 5c).
142 These data indicate that the region that encompasses the D614G mutation is not immunodominant or
143 does not affect the antigenicity of epitopes at or near this site. We also examined whether antibodies
144 targeting the RBD of the spike protein cross-reacted with the RBD proteins of other pandemic threat
145 coronaviruses, including SARS-CoV-1 and Middle East respiratory syndrome (MERS) CoV. We found
146 a positive correlation between antibody titers against the SARS-CoV-2 RBD and the SARS-CoV-1
147 RBD, but not the MERS-CoV RBD (Fig. 5d and e). When divided by responder groups (Fig. 2 and 3),
148 subjects in the high and mid responder groups had elevated titers against the SARS-CoV-1 RBD (Fig.

149 5f and g). These data show that subjects who mounted a larger response against the SARS-CoV-2
150 spike protein additionally mounted a larger antibody response against conserved epitopes that cross-
151 react with closely related coronaviruses.

152 Together, our study demonstrates that severity of SARS-CoV-2 infection is associated with an
153 increase in the magnitude and breadth of the ensuing humoral immune response. Notably, we
154 identified the antibody response is largely mounted against the spike and N proteins, with the
155 magnitude and kinetics of the anti-N protein antibody response outpacing the antibody response
156 against spike. Although both proteins are highly expressed by coronaviruses, there is much more N
157 protein as it encapsulates the whole viral genomic RNA, which is nearly 30 kb in size. As N protein
158 dimer is projected to bind about 30 bp¹², there are likely 1000+ N proteins per virion. In sharp contrast,
159 there are only ~26 spike trimers per virion⁸, suggesting the immunodominance towards N protein may
160 be related to antigen burdens. Likewise, subjects with more severe disease likely have increased viral
161 titers and free antigen in the lung lumen and draining lymph nodes, which could lead to increased
162 antibody titers against nearly all antigens tested. Therefore, epitope spreading of the antibody
163 response may be a factor of the amount of SARS-CoV-2 antigen present.

164 Subjects also mounted an antibody response against the accessory protein ORF8. ORF8 has
165 immunoregulatory properties including the ability to limit type I interferon responses^{13,14} and
166 downregulate MHC-I presentation to CD8 T cells¹⁵. Antibodies targeting ORF8 may limit these
167 immunoregulatory properties, which could improve the host immune response and achieve better
168 clinical disease outcomes. Additionally, we identified antibodies against non-structural proteins
169 involved in viral replication, although antibodies against these antigens are unlikely to provide
170 protection, as these antibodies targeting NSPs would need to be inside of a live cell while virus is
171 replicating. Whether antibodies targeting discrete viral antigens other than the spike are neutralizing,
172 have Fc-mediated effector functions, or are protective during infection remains to be determined.

173 Our study revealed acutely infected subjects who mounted higher antibody response relative
174 to mid and low responder clusters tended to have higher pneumonia severity scores. Consistent with
175 this notion, convalescent subjects who had higher antibody titers were those subjects who had a more

176 severe infection. A recent report identified that subjects who succumbed to COVID-19 tended to
177 mount a larger antibody response against N protein relative to the spike, whereas convalescent
178 subjects tended to focus their antibody response on the spike protein¹⁶. However, our study identified
179 that subjects generally had similar antibody responses against the N protein and spike, and infection
180 severity was linked to an increase in antibody responses against both the spike and N protein.
181 Ultimately, our findings on the relationship between infection severity and increased titers against the
182 spike is consistent with a recent surveillance study performed in Iceland⁶.

183 The best clinical predictors of the magnitude of the antibody responses and epitope spreading
184 within our convalescent cohort were age, sex, and hospitalization. Strikingly, the median age of the
185 high responder cluster was 10+ years greater than the mid and low responder clusters (48 years vs.
186 36 and 38, respectively). Older adults are more likely to be symptomatic and hospitalized with SARS-
187 CoV-2 infection^{17,18}, suggesting increased disease severity and sustained viral titers over a longer
188 period of time could lead to greater antibody titers against multiple viral antigens. Similarly, males
189 were more likely to be segregated into the higher responder group despite the common finding that
190 females generally mount higher antibody responses upon other viral infections and upon
191 vaccination¹⁹. Although there is no difference in incidence of COVID-19 in men and women, men have
192 a higher morbidity and mortality rate than women^{20,21} and likely experience increased viral titers and
193 antigen persistence. Altogether, disease severity is the main clinical predictor of the magnitude of the
194 antibody response mounted against SARS-CoV-2, as men and older adults are more likely to be
195 hospitalized with COVID-19. It remains to be determined whether subjects with more severe disease
196 are more likely to be protected from reinfection with SARS-CoV-2.

197 Together, our data indicate more severe infection is linked to a larger magnitude of circulating
198 antibody and MBC response and increased viral antigen binding breadth across different viral
199 antigens. CD4 T cells are critical for driving antibody responses by mediating germinal center
200 selection of antigen specific B cells. Notably, CD4 T cells targeting multiple SARS-CoV-2 antigens
201 and the magnitude of the CD4 T cell response positively correlate with SARS-CoV-2 specific antibody
202 responses^{22,23}. Moreover, subjects with more severe disease demonstrate an increased breadth and

203 magnitude of the memory CD4 T cell response²³, which could lead to the larger and broader antibody
204 response of subjects with more severe infection, as observed in our study. The increase in the
205 magnitude of the antibody response and MBC response in subjects with more severe infection could
206 be due to increased CD4 T cell responses, although this was not directly tested in our study.
207 However, subjects who succumbed to SARS-CoV-2 infection demonstrated a loss of germinal centers
208 and CD4 T follicular helper cells²⁴. These data in conjunction with our study suggest that an
209 immunological balance will be needed to drive a sufficient secreted antibody response, MBC
210 differentiation, and memory T cell responses that could provide robust protection from reinfection
211 while preventing significant morbidity and mortality associated with SARS-CoV-2 infection.

212 **Methods**

213 **Study cohorts**

214 All studies were performed with the approval of the University of Chicago institutional review board
215 and University of Chicago and University of Wisconsin-Madison institutional biosafety committees.
216 Plasma samples from the acutely infected cohort were collected as residual samples submitted to the
217 University of Chicago Medicine Clinical Laboratories. Convalescent subjects were recruited to donate
218 one unit of blood for a convalescent plasma transfusion study, identified as clinical trial
219 NCT04340050. 3 ml of blood and the leukoreduction filter were provided to the Wilson laboratory. All
220 subjects in the acute and convalescent cohorts had PCR-confirmed SARS-CoV-2 infections.

221 **Recombinant proteins**

222 Plasmids for the SARS-CoV-2 RBD and spike were provided by Dr. Florian Krammer at Icahn School
223 of Medicine at Mount Sinai, and recombinant proteins were expressed in-house in HEK293F cells.
224 D614G spike protein, SARS-CoV-1 RBD, and MERS-CoV RBD were generated in-house and
225 expressed in HEK293F cells. ORF7a, ORF8, and full-length N proteins were cloned from the 2019-
226 nCoV/USA-WA1/2020 SARS-CoV-2 strain at Washington University. Proteins were expressed in
227 *Escherichia coli*, with N protein purified as a soluble protein and ORF7a and ORF8 oxidatively
228 refolded from inclusion bodies. NSP antigens and the RNA-binding domain of N protein were provided
229 by Dr. Andrzej Joachimiak at the Center for Structural Genomics of Infectious Diseases at the
230 University of Chicago and Argonne National Laboratory and were expressed in *Escherichia coli*.

231 **Enzyme-linked immunosorbent assay (ELISA)**

232 ELISAs performed in this study were adapted from previously established protocols^{25,26}. Plasma
233 samples were heat-inactivated for 1 hour at 56°C. High protein-binding microtiter plates (Costar) were
234 coated with recombinant antigens at 2 g/ml in phosphate-buffered saline (PBS) overnight at 4°C.
235 Plates were washed with PBS 0.05% Tween and blocked with 200 l PBS 0.1% Tween + 3% milk
236 powder for 1 hour at room temperature. Plasma samples were serially diluted in PBS 0.1% Tween +
237 1% milk powder. Plates were incubated with serum dilutions for 2 hours at room temperature.
238 Horseradish peroxidase (HRP)-conjugated goat anti-human Ig secondary antibody diluted in PBS

239 0.1% Tween + 1% milk powder was used to detect binding of antibodies, and after a 1-hour
240 incubation, plates were developed with 100 µl SigmaFast OPD solution (Sigma-Aldrich), with
241 development reaction stopped after 10 minutes using 50 µl 3M HCl. Absorbance was measured at
242 490 nm on a microplate spectrophotometer (BioRad). To detect binding of specific antibody isotypes
243 and subclasses, ELISAs were performed using alternate secondary antibodies (Sigma-Aldrich;
244 Jackson ImmunoResearch; Southern Biotech). End point titers were extrapolated from sigmoidal 4PL
245 (where X is log concentration) standard curve for each sample. Limit of detection (LOD) is defined as
246 the mean plus 2-8 S.D. (depending on antigen) of the O.D. signal recorded using plasma from SARS-
247 CoV-2 negative human subjects. All calculations were performed in Prism 8 (GraphPad).

248 **Neutralization assays**

249 Neutralization assays were performed by a viral cytopathic effect assay (CPE) using the SARS-CoV-
250 2/UW-001/Human/2020/Wisconsin (UW-001), which was isolated from a mild human case in
251 Wisconsin. Plasma was diluted 1:5 and serially diluted 2-fold and was mixed with an equal volume of
252 virus (100 plaque-forming units) for a starting dilution of 1:10. The plasma/virus mixture was incubated
253 for 30 minutes at 37°C and added to TMPRSS2-expressing Vero E6 cells grown in 1x minimum
254 essential medium (MEM) supplemented with 5% FCS. Cells were incubated with plasma/virus mixture
255 for 3 days, and then were fixed, stained, and analyzed. CPE was observed under an inverted
256 microscope, and neutralization titers were determined as the highest serum dilution that completely
257 prevented CPE.

258 **Memory B cell stimulations and enzyme-linked immunospot assays (ELISpot)**

259 MBC stimulations were performed on peripheral blood mononuclear cells (PBMCs) collected from
260 subjects in the convalescent cohort. To induce MBC differentiation into antibody secreting cells, 1x10⁶
261 PBMCs were stimulated with 10 ng/ml Lectin Pokeweed Mitogen (Sigma-Aldrich), 1/100,000 Protein A
262 from *Staphylococcus aureus*, Cowan Strain (Sigma-Aldrich), and 6 µg/ml CpG (Invitrogen) in
263 complete RPMI in an incubator at 37°C/5% CO₂ for 5 days. After stimulation, cells were counted and
264 added to ELISpot white polystyrene plates (Thermo Fisher) coated with 4 µg/ml of SARS-CoV-2 spike

265 that were blocked with 200 μ l of complete RPMI. ELISpot plates were incubated with cells for 16
266 hours overnight in an incubator at 37°C/5% CO₂. After the overnight incubation, plates were washed
267 and incubated with anti-IgG-biotin and/or anti-IgA-biotin (Mabtech) for 2 hours at room temperature.
268 After secondary antibody incubation, plates were washed and incubated with streptavidin-alkaline
269 phosphatase (Southern Biotech) for 2 hours at room temperature. Plates were washed and developed
270 with NBT/BCIP (Thermo Fisher Scientific) for 2-10 minutes, and reactions were stopped by washing
271 plates with distilled water and allowed to dry overnight before counting. Images were captured with
272 Immunocapture 6.4 software (Cellular Technology Ltd.), and spots were manually counted.

273 **Infection Severity Scoring and CURB-65 scoring**

274 For the acutely infected cohort, CURB-65⁹ scores were calculated based on confusion, blood urea
275 nitrate levels, respiratory rate, blood pressure, and age of subjects. For the convalescent cohort, we
276 designed a severity scoring system (Supplemental Table 5) based on presence of 12 symptoms,
277 duration of symptoms, and hospitalization, with a maximum of 35 points possible. Symptoms were
278 scored based on presence or absence of 12 symptoms, severity (mild or moderate) of symptoms, with
279 a possibility of 17 points. Duration of symptoms was broken down based on the number of weeks of
280 symptoms. Hospitalized subjects were broken down based on oxygen supplementation and intensive
281 care unit (ICU) admission. The criteria for scoring and the classification of certain scores (mild,
282 moderate, severe, and critical infection) were determined before analyzing the data.

283 **Heatmaps, hierarchical clustering, and statistical analysis**

284 Heatmaps were generated by 'pheatmap' *R* package (version 1.0.12). Features and subjects were
285 clustered by the hierarchical clustering method implemented in the 'pheatmap' *R* package. Principal
286 component analyses (PCA) were performed using 'factoextra' *R* package (version 1.0.7). Subjects
287 were then visualized by their first two principal components (PC1 and PC2) on a 2D map. All
288 statistical analysis was performed using Prism software (Graphpad Version 8), JMP (SAS Institute
289 Version 15), or *R* (version 3.6.3). Specific tests for statistical significance used are indicated in the
290 corresponding figure legends. *P* values less than or equal to 0.05 were considered statistically
291 significant.

292 **Acknowledgements**

293 This project was funded in part by the National Institute of Allergy and Infectious Diseases; National
294 Institutes of Health grant numbers U19AI082724 (P.C.W.), U19AI109946 (P.C.W.), U19AI057266
295 (P.C.W.). This work was also partially supported by the National Institute of Allergy and Infectious
296 Diseases Collaborative Influenza Vaccine Innovation Centers (CIVIC; 75N93019C00051, F.K. and
297 P.C.W.), and the Centers of Excellence for Influenza Research and Surveillance (CEIRS)
298 HHSN272201400008C (F.K.) and by the National Institute of Allergy and Infectious Diseases,
299 National Institutes of Health, Department of Health and Human Services, under Contract
300 HHSN272201700060C (A.J., D.F.). This work was also supported by the National Heart, Lung, Blood
301 Institute award T32HL007605-35 (J.J.G.). We thank Shruti Kamath for assisting in analyzing CURB-
302 65 scoring data for the acutely infected cohort. We would like to thank Dr. Robert Jedrzejczak for help
303 with cloning, expression, and purification of SARS CoV-2 proteins. We are thankful to all subjects who
304 participated in this study.

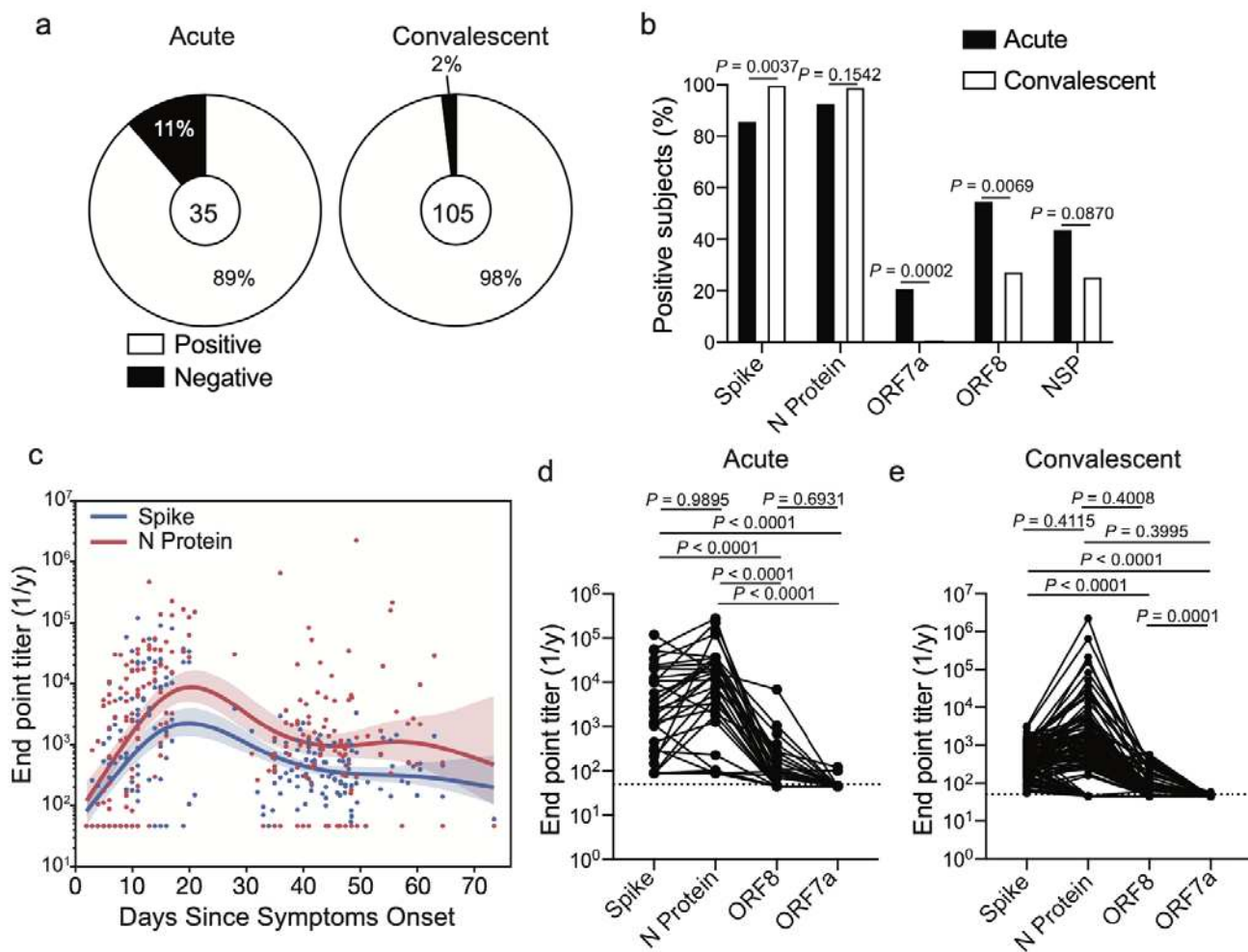
305 **Author Contributions**

306 J.J.G. designed and performed experiments, analyzed the data, and wrote the manuscript. O.S. and
307 J.W. performed experiments, analyzed the data, and wrote the manuscript. S.C., N.Y.Z., H.U., M.H.,
308 Y.N.D., C.A.N, and P.D.H. generated recombinant antigens. J.J.G., S.C., N.Y.Z., H.U., C.T.S., and
309 H.L.D. processed convalescent blood samples. J.J.G., O.S., and C.T.S. processed samples from
310 acutely infected subjects. J.J.G., J.W., S.C., C.T.S., and H.L.D. performed and analyzed ELISpot
311 assays. L.L. performed hierarchical clustering and PCA analyses. P.H. and Y.K. performed
312 neutralization assays. J.J.G., W.D.M., and M.L.M. designed the scoring system for convalescent
313 subjects. M.J., K.S., J.S.D., and M.L.M. orchestrated convalescent plasma study. F.K., D.H.F., and
314 A.J. provided recombinant antigens or plasmids to express recombinant antigens. V.T. provided
315 samples from acutely infected subjects and helped analyze data. P.C.W. supervised the work. All
316 authors edited the manuscript.

317 **Declaration of Interests**

318 The authors declare no competing interests.

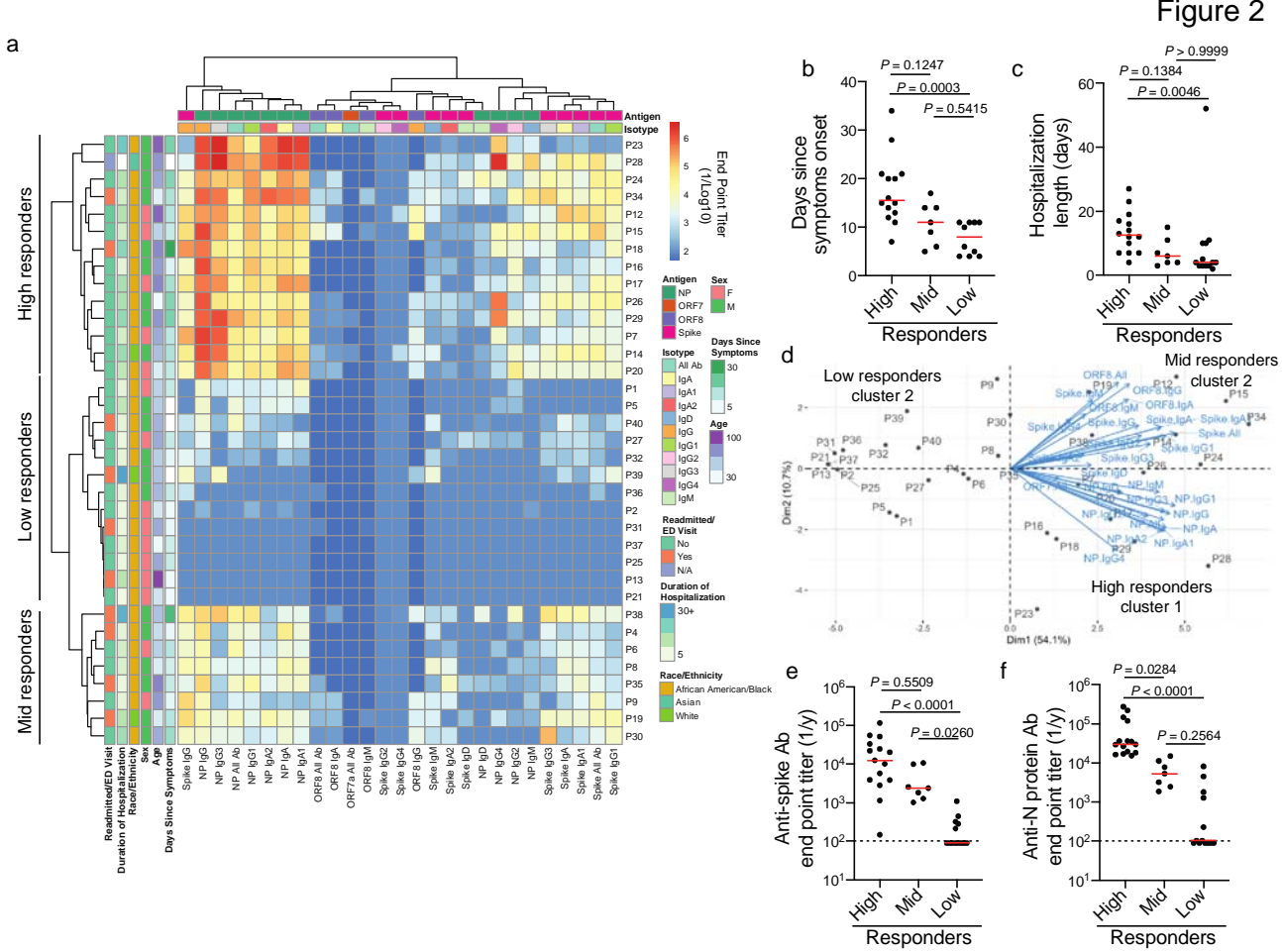
Figure 1



319

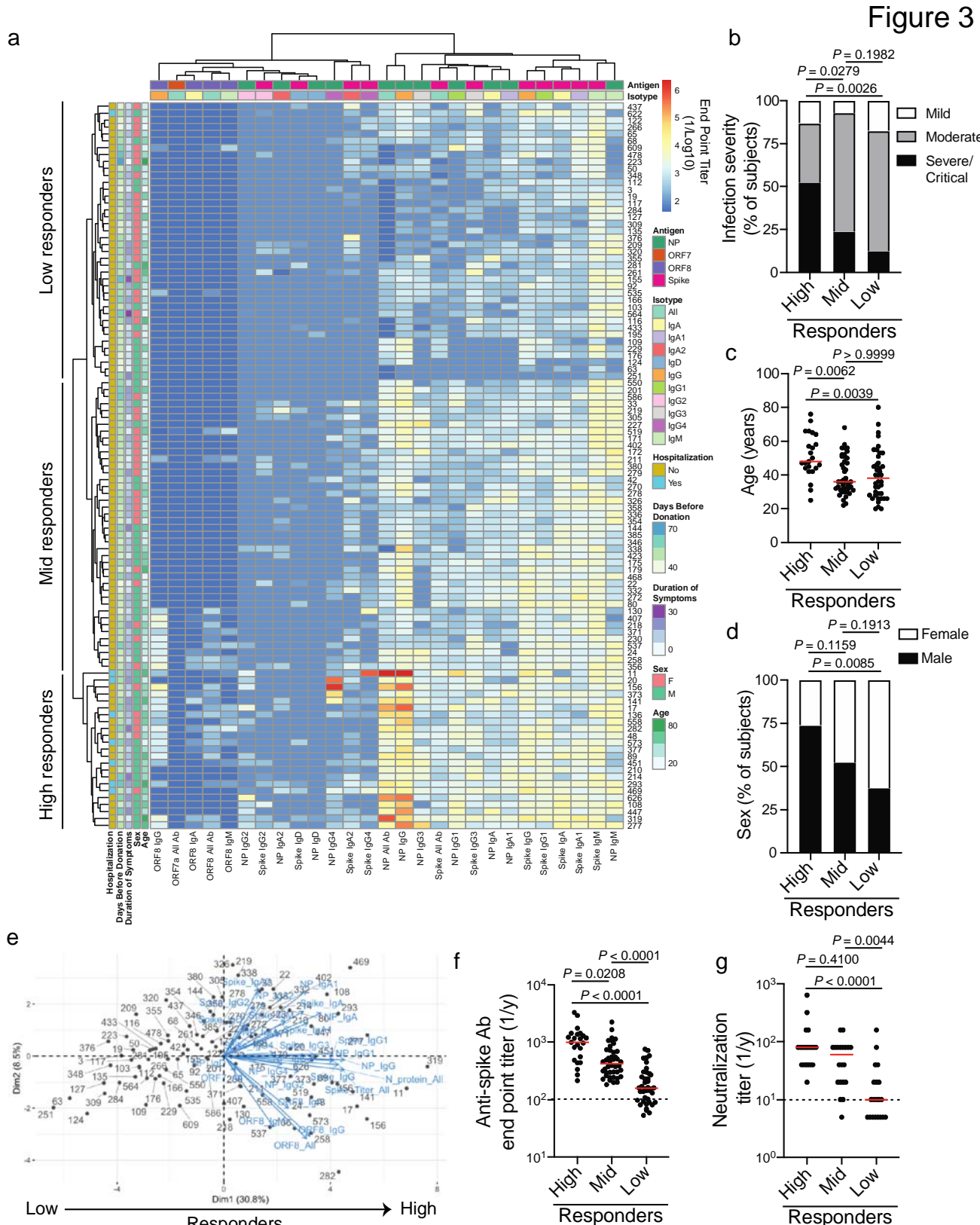
320 **Fig. 1: Antibody specificity and kinetics in SARS-CoV-2 infected subjects.** **a**, Proportion of
321 subjects in the acutely infected and convalescent cohorts who have seroconverted to one or more
322 SARS-CoV-2 antigens. Number in center represents the number of subjects tested in each cohort. **b**,
323 Proportion of subjects in the acutely infected (n=35) and convalescent (n=105) cohorts binding spike,
324 N protein, ORF7a, ORF8, or at least one NSP antigen. **c**, Kinetics of plasma antibodies against the
325 spike and N protein based on the start of symptoms. Data are pooled from the acute (n=117) and
326 convalescent cohorts (n=105). Lines represent the fitted lines for spike and N protein titers and the
327 shaded region indicates confidence of fit of the fitted line. **d** and **e**, end point titers of antibodies
328 targeting spike, N protein, ORF7a, and ORF8 in the acutely infected cohort (**d**; n=35) and
329 convalescent cohort (**e**; n=105). Lines connect titers across one subject. Data in **b** were analyzed

330 using Fisher's exact tests for statistical analyses. Data in **d** and **e** were analyzed using paired non-
331 parametric Friedman tests. Dashed lines in **d** and **e** are the limit of detection.
332



333

334 **Fig. 2: Acutely infected subjects with longer hospitalizations have a higher antibody response**
335 **against N protein. a**, Heatmap of hierarchical clustering of acutely infected subjects (n=35) based on
336 antibody binding specificity and antibody isotype/subclass. Subjects clustered into three distinct
337 clusters: high (n=15), mid (n=7), and low (n=13) responders. **b** and **c**, days since symptom onset (**b**)
338 and length of hospitalization (**c**) amongst subjects in the high, mid and low responder clusters. **d**, PCA
339 biplot of subjects clustering based on distinct antibody binding features. **e** and **f**, total antibody titers
340 against the spike (**e**) and N protein (**f**) amongst the high, mid, and low responder clusters. Data in **b**,
341 **c**, **e**, and **f** were analyzed using unpaired non-parametric Kruskal-Wallis tests. Dashed lines in **e** and **f**
342 are the limit of detection. Bars in **b**, **c**, **e**, and **f** represent the median.

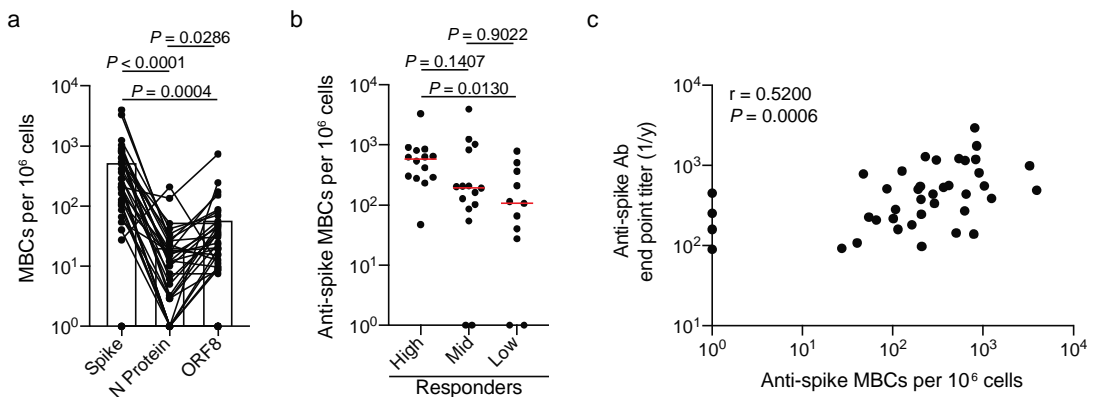


343

344 **Fig. 3: Convalescent subjects with higher antibody responses against multiple SARS-CoV-2**
345 **antigens tended to have a more severe infection. a, Heatmap of hierarchical clustering of**

346 convalescent subjects (n=105) based on antibody binding specificity and antibody isotype/subclass.
347 Subjects clustered into three distinct clusters: high (n=23), mid (n=42), and low (n=40) responders. **b-**
348 **d**, infection severity (**b**), age (**c**) and sex (**d**) of subjects in the high, mid and low responder clusters. **e**,
349 PCA biplot of subjects clustering based on distinct antibody binding features. **f**, Total antibody titers
350 against the spike amongst the high, mid, and low responder clusters. **g**, Neutralization titer, as
351 determined by viral cytopathic effect, of 20 randomly selected samples from each of the high, mid,
352 and low responder clusters. Data in **f** and **g** were analyzed using unpaired non-parametric Kruskal-
353 Wallis tests. For **b-d**, data were analyzed using Fisher's exact tests. Dashed lines in **f** and **g** are the
354 limit of detection. Bars in **f** and **g** represent the median.

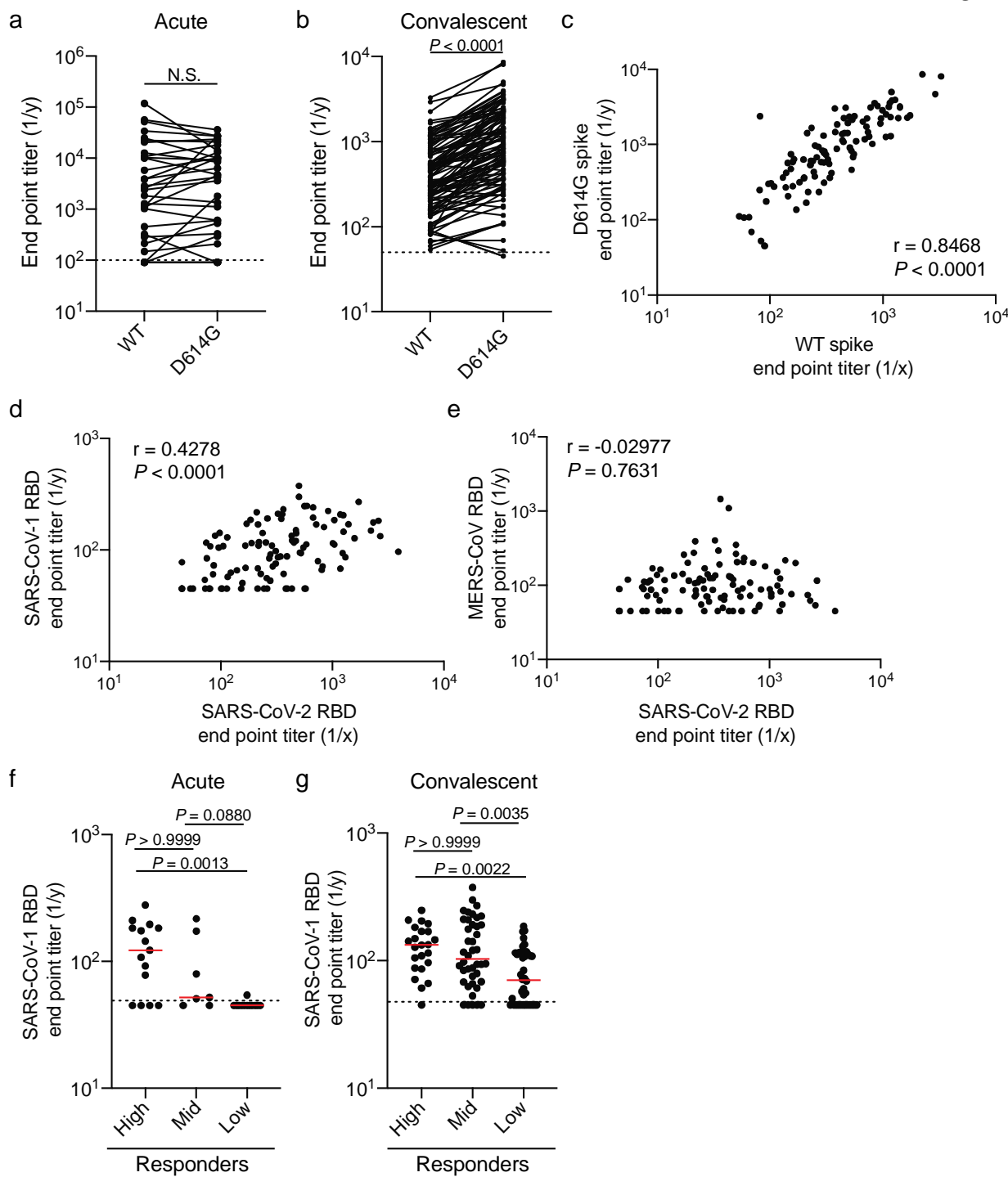
Figure 4



355
356

357 **Fig. 4: MBC response is largely driven against the spike. a and b,** PBMCs from convalescent
358 donors were polyclonally stimulated and ELISpots were performed to assess the number of antigen-
359 specific MBCs. **a**, Number of MBCs (antigen-specific MBCs per 10^6 cells) targeting the spike, N
360 protein, or ORF8 (n=36). Lines connect antigen-specific MBCs across subjects. **b**, Number of spike
361 targeting MBCs amongst the high (n=14), mid (n=15), and low responder (n=11) clusters. **c**,
362 Spearman correlation of the number of anti-spoke MBCs and anti-spoke end point titers by individual
363 (n=40). Data in **a** were analyzed using paired non-parametric Friedman tests. Data in **b** were analyzed
364 using unpaired non-parametric Kruskal-Wallis tests. Data in **c** were analyzed by a non-parametric
365 two-tailed Spearman correlation.

Figure 5



366

367 **Fig. 5: Antibody cross-reactivity to G614 spike mutant and SARS-CoV-1 and MERS-CoV RBD. a**
 368 and **b**, End point titers of antibodies binding to the WT (D614) and mutant (D614G) SARS-CoV-2
 369 spike protein from the acute (**a**; n=35) and convalescent (**b**; n=105) cohorts. **c**, Correlation of end
 370 point titers against the WT (D614) and mutant (D614G) spike from the convalescent cohort (n=105). **d**

371 and **e**, correlation between SARS-CoV-2 RBD end point titers and SARS-CoV-1 RBD (**d**) or MERS-
372 CoV RBD (**e**) end point titers from convalescent subjects (n=105). **f** and **g**, SARS-CoV-1 RBD end
373 point titers amongst the high, mid, and low responder clusters from the acutely infected cohort (**f**; high
374 n=23, mid n=42, and low n=40) and the convalescent cohort (**g**; high n=23, mid n=42, and low n=40).
375 Data in **a** were analyzed using a two-tailed Wilcoxon matched-pairs signed rank test. Data in **b** were
376 analyzed using a two-tailed paired t-test. For **c-e**, data were analyzed using a two-tailed Pearson
377 correlation. Data in **f** and **g** were analyzed using unpaired non-parametric Kruskal-Wallis tests.
378 Dashed lines in **a**, **b**, **f** and **g** are the limit of detection. Bars in **f** and **g** represent the median.

379 References

380 1 Walls, A. C. *et al.* Structure, Function, and Antigenicity of the SARS-CoV-2 Spike
381 Glycoprotein. *Cell* **181**, 281-292 e286, doi:10.1016/j.cell.2020.02.058 (2020).

382 2 Letko, M., Marzi, A. & Munster, V. Functional assessment of cell entry and receptor usage for
383 SARS-CoV-2 and other lineage B betacoronaviruses. *Nat Microbiol* **5**, 562-569,
384 doi:10.1038/s41564-020-0688-y (2020).

385 3 Amanat, F. & Krammer, F. SARS-CoV-2 Vaccines: Status Report. *Immunity* **52**, 583-589,
386 doi:10.1016/j.jimmuni.2020.03.007 (2020).

387 4 Chan, J. F. *et al.* Genomic characterization of the 2019 novel human-pathogenic coronavirus
388 isolated from a patient with atypical pneumonia after visiting Wuhan. *Emerg Microbes Infect* **9**,
389 221-236, doi:10.1080/22221751.2020.1719902 (2020).

390 5 Madariaga, M. L. L. *et al.* Clinical predictors of donor antibody titer and correlation with
391 recipient antibody response in a COVID-19 convalescent plasma clinical trial. *medRxiv*,
392 2020.2006.2021.20132944, doi:10.1101/2020.06.21.20132944 (2020).

393 6 Gudbjartsson, D. F. *et al.* Humoral Immune Response to SARS-CoV-2 in Iceland. *N Engl J
394 Med*, doi:10.1056/NEJMoa2026116 (2020).

395 7 Rodda, L. B. *et al.* Functional SARS-CoV-2-specific immune memory persists after mild
396 COVID-19. *medRxiv*, doi:10.1101/2020.08.11.20171843 (2020).

397 8 Ke, Z. *et al.* Structures and distributions of SARS-CoV-2 spike proteins on intact virions.
398 *Nature*, doi:10.1038/s41586-020-2665-2 (2020).

399 9 Lim, W. S. *et al.* Defining community acquired pneumonia severity on presentation to hospital:
400 an international derivation and validation study. *Thorax* **58**, 377-382,
401 doi:10.1136/thorax.58.5.377 (2003).

402 10 Korber, B. *et al.* Tracking Changes in SARS-CoV-2 Spike: Evidence that D614G Increases
403 Infectivity of the COVID-19 Virus. *Cell*, doi:10.1016/j.cell.2020.06.043 (2020).

404 11 Zhang, L. *et al.* The D614G mutation in the SARS-CoV-2 spike protein reduces S1 shedding
405 and increases infectivity. *bioRxiv*, doi:10.1101/2020.06.12.148726 (2020).

406 12 Huang, Q. *et al.* Structure of the N-terminal RNA-binding domain of the SARS CoV
407 nucleocapsid protein. *Biochemistry* **43**, 6059-6063, doi:10.1021/bi036155b (2004).

408 13 Li, J. Y. *et al.* The ORF6, ORF8 and nucleocapsid proteins of SARS-CoV-2 inhibit type I
409 interferon signaling pathway. *Virus Res* **286**, 198074, doi:10.1016/j.virusres.2020.198074
410 (2020).

411 14 Lei, X. *et al.* Activation and evasion of type I interferon responses by SARS-CoV-2. *Nat
412 Commun* **11**, 3810, doi:10.1038/s41467-020-17665-9 (2020).

413 15 Zhang, Y. *et al.* The ORF8 Protein of SARS-CoV-2 Mediates Immune Evasion through
414 Potently Downregulating MHC-I. *bioRxiv*, 2020.2005.2024.111823,
415 doi:10.1101/2020.05.24.111823 (2020).

416 16 Atyeo, C. *et al.* Distinct Early Serological Signatures Track with SARS-CoV-2 Survival.
417 *Immunity*, doi:10.1016/j.jimmuni.2020.07.020 (2020).

418 17 Davies, N. G. *et al.* Age-dependent effects in the transmission and control of COVID-19
419 epidemics. *Nat Med*, doi:10.1038/s41591-020-0962-9 (2020).

420 18 Tenforde, M. W. *et al.* Characteristics of Adult Outpatients and Inpatients with COVID-19 - 11
421 Academic Medical Centers, United States, March-May 2020. *MMWR Morb Mortal Wkly Rep*
422 **69**, 841-846, doi:10.15585/mmwr.mm6926e3 (2020).

423 19 Klein, S. L. & Flanagan, K. L. Sex differences in immune responses. *Nat Rev Immunol* **16**, 626-
424 638, doi:10.1038/nri.2016.90 (2016).

425 20 Chakravarty, D. *et al.* Sex differences in SARS-CoV-2 infection rates and the potential link to
426 prostate cancer. *Commun Biol* **3**, 374, doi:10.1038/s42003-020-1088-9 (2020).

427 21 Jin, J. M. *et al.* Gender Differences in Patients With COVID-19: Focus on Severity and
428 Mortality. *Front Public Health* **8**, 152, doi:10.3389/fpubh.2020.00152 (2020).

429 22 Grifoni, A. *et al.* Targets of T Cell Responses to SARS-CoV-2 Coronavirus in Humans with
430 COVID-19 Disease and Unexposed Individuals. *Cell* **181**, 1489-1501 e1415,
431 doi:10.1016/j.cell.2020.05.015 (2020).

432 23 Peng, Y. *et al.* Broad and strong memory CD4(+) and CD8(+) T cells induced by SARS-CoV-2
433 in UK convalescent individuals following COVID-19. *Nat Immunol*, doi:10.1038/s41590-020-
434 0782-6 (2020).

435 24 Kaneko, N. *et al.* Loss of Bcl-6-Expressing T Follicular Helper Cells and Germinal Centers in
436 COVID-19. *Cell*, doi:10.1016/j.cell.2020.08.025 (2020).

437 25 Amanat, F. *et al.* A serological assay to detect SARS-CoV-2 seroconversion in humans. *Nat
438 Med* **26**, 1033-1036, doi:10.1038/s41591-020-0913-5 (2020).

439 26 Stadlbauer, D. *et al.* SARS-CoV-2 Seroconversion in Humans: A Detailed Protocol for a
440 Serological Assay, Antigen Production, and Test Setup. *Curr Protoc Microbiol* **57**, e100,
441 doi:10.1002/cpmc.100 (2020).

442